Materials Research Proceedings 41 (2024) 2041-2049 https://doi.org/10.21741/9781644903131-225

Numerical simulation of milling operations on flexible composite parts

NUTTE Matthias[1,a*], RIVIÈRE-LORPHÈVRE Edouard[1], DAMBLY Valentin[1], ARRAZOLA Pedro-José[2], LAZOGLU Ismail[3] and DUCOBU François[1]

[1]Machine Design and Production Engineering Lab, Research Institute for Science and Material Engineering, UMONS, Belgium

[2]Mechanical and Manufacturing Department, Faculty of Engineering, Mondragon Unibertsitatea, Loramendi 4, 20500 Arrasate-Mondragón, Spain

[3]Koc University Manufacturing and Automation Research Center, Istanbul 34450, Turkey

[a]Matthias.NUTTE@umons.ac.be

Keywords: Machining, Milling, CFRP, Flexible Parts, Form Error

Abstract. Fiber-reinforced polymers (FRPs) are a widely used and growing material in industry, thanks to their excellent mechanical properties. Manufactured FRPs parts usually have thin walls. These parts also require finishing operations such as edge trimming. Problems like those encountered when machining thin metal parts are also encountered with FRPs: form error, chatter vibrations and poor surface finish. However, the study and numerical modelling of thin FRP parts are not well developed up to now. The aim of this paper is to demonstrate the feasibility of adapting a numerical model for metals to FRPs. The modelling of the shape error during the thinning of a CFRP (Carbon Fiber Reinforced Polymers) part is studied in this paper using a quasi-static analysis. Compared to metals, two adaptations are introduced here for the FRPs. First, the material properties are adapted from isotropic to orthotropic. Secondly, a mechanical model was applied to calculate cutting forces for FRPs. The results of the study show the feasibility of this adaptation and examination of form error in the case of FRPs.

Introduction

Fiber-reinforced polymers (FRPs) are excellent material owning a high strength to weight ratio and the performance of high toughness, good fatigue resistance and shock absorption, and strong designability [1]. However, FRPs forming techniques often result in the production of thin-walled parts. It is therefore important to consider the parts' flexibility when machining them, particularly when milling. On the one hand, the numerical simulation of flexible metal parts has been explored in numerous studies [2–4]. On the other hand, other studies have explored the numerical simulation of the machining of FRPs parts ([1] published a review on this subject in 2021). In addition, some articles, for example [5], have studied subjects already well known for metals, such as chattering, in the case of composites. However, to the authors' knowledge, no article has studied the numerical simulation of milling operations on flexible composite parts. Ciecieląg et al. [6] studied the milling of flexible composite parts, but only experimentally.

To simulate the behaviour of a thin plate during milling, it is necessary to compute the cutting forces. There are 4 categories of models for calculating cutting forces in milling for unidirectional FRPs (UD-FRPs): mechanistic models, macro-mechanical models, micro-mechanical models, and numerical models. Mechanistic models are semi-empirical models. They are the most intuitive method to optimize cutting parameters and tool geometries, but they require a lot of time-consuming experiments to ensure the accuracy and applicability [7]. However, the calculation time after obtaining the cutting coefficients is short. Macro-mechanical models consider the material as an equivalent homogeneous material. They can help to optimize cutting parameters and to reduce

cutting forces as models can describe the interaction "cutting tool/FRP", but they cannot describe the microchip formation process [7]. Micro-mechanical models consider the composite in all its details (fibres and matrix). Compared with macro-mechanical models and mechanistic models, micro-mechanical models can predict the cutting force by the physical essence of cutting of FRPs based on microscopic characteristics of FRPs, but the models need many parameters and details, which are difficult to be calibrated by measurements [7]. Thus, applications of these models have great limitations. Numerical models are mainly based on finite element methods (FEM) [8, 9] (discrete element models (DEM) do exist but are in the minority [10]). The main advantages of these models are that they save a lot of manpower and material resources, and that the cutting process can be described more accurately, but numerical models are limited by computer power and finite element theory [7]. Indeed, these models require more resources and computing time than the other models.

In this study, a quasi-static approach and a mechanistic model are used. This quasi-static approach is intended to deal with form error during chatter-free machining operations. It is used to compute form error (vibration problems are negligible). The dynamic system is considered as purely static to predict deformation during machining [4]. A quasi-static method is used to reduce calculation time compared with full dynamic simulation. To achieve this, the finite element modeling of the thin plate and the modeling of cutting forces for an orthotropic material such as FRPs need to be implemented. A mechanistic cutting forces model will be considered. The aim of this article is to demonstrate the feasibility of studying the form error in CFRPs milling process.

Case study

The case studied is the lateral milling (up or down milling) of a thin unidirectional carbon fiber reinforced polymer (UD-CFRP) laminated plate. It is a plate thinning operation.

The plate, of thickness e, consists of a superposition of plies of thickness e_p. Each ply is made up of unidirectional carbon fiber (represented in blue in Fig. 1) and of matrix in epoxy (surrounding the fibers). The fibers are oriented along the longitudinal axis l. The t axis is transverse to the fibers. The axes l and t form the local frame lt. The fiber orientation angle ψ is the angle between the local frame lt and the global frame XZ (Fig. 1). In this case, the fiber orientation angle ψ is 0°: the fibers are oriented horizontally. The local frames lt of the plies are therefore merged with the global frame XZ.

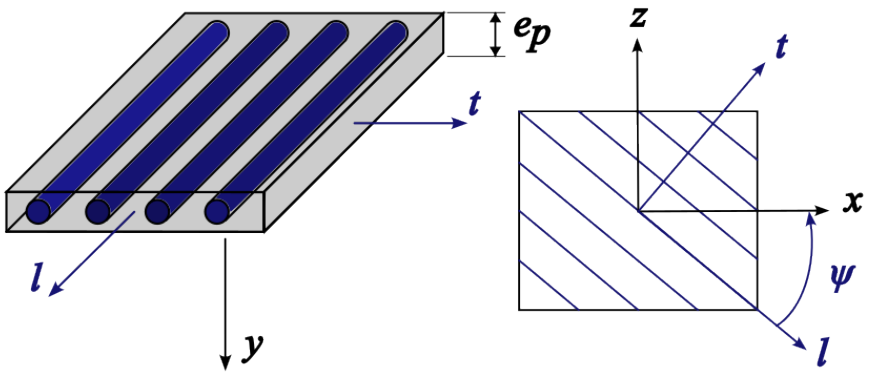

Figure 1: UD-FRP ply, frame convention

The plate, contained in the *XZ* plane, is made up of n plies of thickness e_p (Fig. 2). A cross-section of the plate in the XY plane is shown in Fig. 3. Each ply (shown in a shade of grey in Fig. 2) has a carbon fiber (shown in blue in Fig. 2) oriented along the X axis (since $\psi = 0°$).

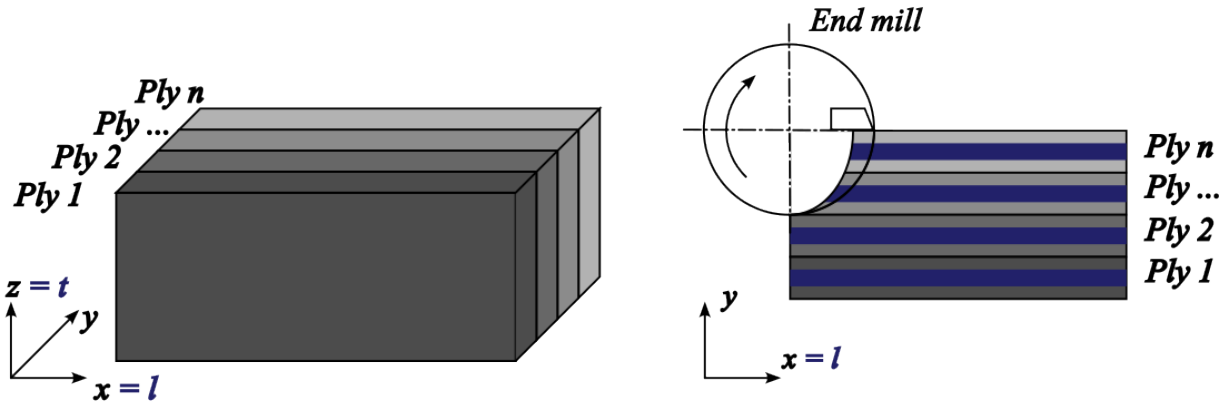

Figure 2: Ply stacking and view in the XY plane of milling

The feed direction is along the *X* axis (Fig. 3). The feed direction is therefore the same as the direction of orientation of the fibers. In other words, the cutter's axis is perpendicular to the fibers' axis for each ply. This is the major assumption of the developed model in link with the cutting forces calculation model. The plate is clamped by its base. The radial depth of cut a_e is less than the thickness of the plate *e*.

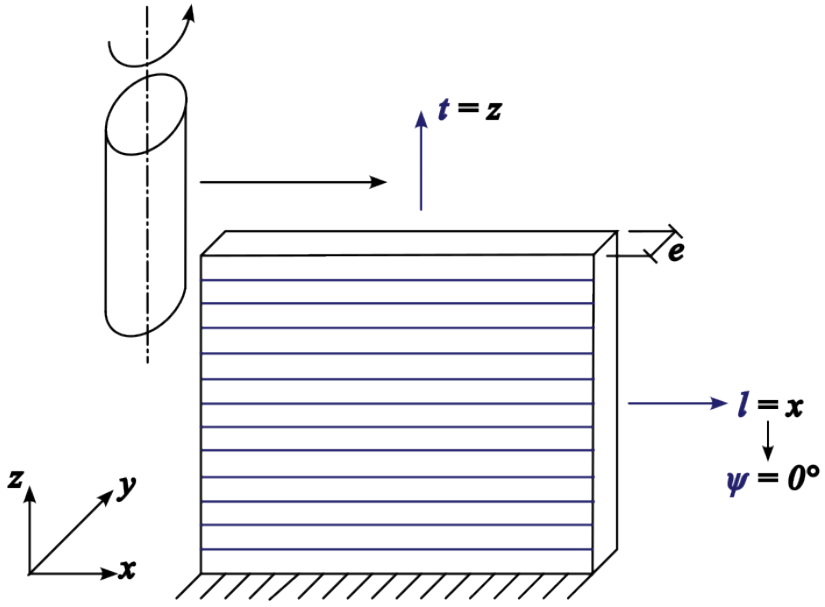

Figure 3: Milling of a thin CFRP laminated plate

Modelling of the milling process

The milling model for the case studied is based on a milling simulator for isotropic metallic thin plates. This simulator named DyStaMill was developed by Prof. Rivière-Lorphèvre and is presented in Huynh et al. [11]. It was therefore necessary to adapt this simulator for the case study: machining a thin composite plate. Two essential points had to be adapted:

1. The finite element thin plate model for an orthotropic material such as FRPs.
2. The cutting model for unidirectional composite milling.

Mechanical properties of CFRPs: The mechanical properties of a UD-FRP ply can be expressed directly as a function of the mechanical characteristics of the fibres (*f*) and the matrix (*m*) (Eq. 1-5) and the volume of fiber (V_f) using mixing laws [12]. The modulus of elasticity in the fibre direction E_l and in the transverse direction E_t are expressed in Eq. 1 and Eq. 2. These properties are a function of the modulus of elasticity of the fibre in the longitudinal $E_{f,l}$ and transverse $E_{f,t}$ directions and the modulus of elasticity of the matrix E_m.

$$E_l = E_{f,l}V_f + E_m(1 - V_f) \tag{1}$$

$$E_t = \frac{E_m}{(1-V_f) + \frac{E_m}{E_{f,t}}V_f} \tag{2}$$

The Poisson's ratio υ_{lt} is expressed in Eq. 3. It is a function of the Poisson's ratio of the fibre υ_f and the matrix υ_m.

$$\upsilon_{lt} = \upsilon_f V_f + \upsilon_m(1 - V_f) \tag{3}$$

By symmetry property, the Poisson's ratio υ_{tl} is expressed in Eq. 4:

$$\upsilon_{tl} = \upsilon_{lt}\frac{E_t}{E_l} \tag{4}$$

The shear modulus G_{lt} is expressed in Eq. 5. It is a function of the fibre shear modulus $G_{f,lt}$ and the matrix shear modulus G_m.

$$G_{lt} = \frac{G_m}{(1-V_f) + \frac{G_m}{G_{f,lt}}V_f} \tag{5}$$

Dynamic response of thin orthotropic plate: The finite element model developed in DyStaMill is based on the thin plate model presented by Zienkiewicz [13]. This finite element model allows to compute the dynamic response of the thin plate subjected to bending. The main assumption is to consider only the flexibility of the workpiece. Indeed, the CNC milling machine has a greater rigidity than the workpiece. The dynamic behavior of the tool/CNC milling machine can therefore be neglected. 2D plate type elements are used. They are composed of four nodes with three degrees of freedom for each of them (out of plane displacements and bending).

The description of the dynamic system can be expressed in a global equation (Eq. 6) and can be solved as explained in [4] :

$$[M]\{\ddot{x}\} + [C]\{\dot{x}\} + [K]\{x\} = \{f\} \tag{6}$$

[*M*], [*C*] and [*K*] are mass, damping and rigidity matrices, {*x*} is the vector containing configuration parameters (the three degrees of freedom per node as described previously) and {*f*} the forces acting on the system.

For a quasi-static analysis, the equation becomes (Eq. 7):

$$[K]\{x\} = \{f\} \tag{7}$$

It is possible to build the stiffness matrix K for a rectangular element (Eq. 8) [13] :

$$K = \frac{1}{60ab}L\{D_xK_1 + D_zK_2 + D_1K_3 + D_{xz}K_4\}L \tag{8}$$

a and b are related to the dimensions of the rectangular element. The matrices K_1, K_2, K_3, K_4 and L are intermediate matrices in the construction of the stiffness matrix K. D_x, D_z, D_{xz} and D_1 are elements of the elasticity matrix D_{XZ} in the global reference XZ (fig. 3). The matrix D_{XY} is defined for an orthotropic material by Eq. 9 [14] :

$$D_{xz} = \begin{bmatrix} D_x & D_{1,xz} & 0 \\ D_{1,xz} & D_z & 0 \\ 0 & 0 & D_{xz} \end{bmatrix} \quad (9)$$

The elasticity matrix D_{lt} of the ply in its local frame lt is expressed by Eq. 10. In the case studied, as the fibre orientation angle ψ is zero, the elasticity matrices in the local and global reference frames are identical.

$$D_{lt} = D_{xz} = \begin{bmatrix} D_l & D_{1,lt} & 0 \\ D_{1,lt} & D_t & 0 \\ 0 & 0 & D_{lt} \end{bmatrix} \quad (10)$$

The components of the elasticity matrix are defined by Eq. 11. These expressions are valid for the case of a laminate of thickness e with all its plies oriented horizontally (Fig. 3).

$$D_l = \frac{E_l}{1-\upsilon_{tl}\upsilon_{lt}}\frac{e^3}{12}\ ,\ D_t = \frac{E_t}{1-\upsilon_{tl}\upsilon_{lt}}\frac{e^3}{12}\ ,\ D_{lt} = G_{lt}\frac{e^3}{12}\ ,\ D_{1,lt} = \frac{\upsilon_{lt}E_l}{1-\upsilon_{tl}\upsilon_{lt}}\frac{e^3}{12}, \quad (11)$$

Cutting force model for composite material: The new mechanistic cutting forces model implemented in the DyStaMill software is the model developed by Mullin et al. [15]. The expression of the cutting force applied in radial (Eq. 12) and tangential (Eq. 13) directions is similar to Altintas' model [16].

$$dF_r(\varphi) = K_{rc}(\beta)\, h\, dz + K_{re}(\beta)\, dS \quad (12)$$

$$dF_t(\varphi) = K_{tc}(\beta)\, h\, dz + K_{te}(\beta)\, dS \quad (13)$$

Altintas' model considers two contributions in both directions (radial r and tangential t). The first ones are related to friction in the primary shear zone: a function of the radial and tangential cutting force coefficient, respectively K_{rc} and K_{tc}, the instantaneous uncut chip thickness h and the height of a tool edge dz. The second ones consider the effect of friction in the secondary shear zone and is a function of the radial and tangential edge force coefficient, respectively K_{re} and K_{te}, and the local segment dS of the cutting edge. However, cutting (K_{rc} and K_{tc}) and edge (K_{re} and K_{te}) coefficients vary according to the instantaneous fiber cutting angle β (Eq. 14).

$$K_{ij}(\beta) = C_0^{ij} + C_1^{ij}\, cos(2\beta) + S_1^{ij}\, sin(2\beta)\ \ with\ i = t,r\ and\ j = c,e \quad (14)$$

The method for identifying the coefficients and their values is given in [15]. These values are only valid for the tool/material pair used in [15]: a 2-flute Tungsten Carbide end mill with 9.525 mm (3/8 inch) diameter and 3° normal rake angle and UD-CFRP (alternating 0° and 90° directions).

Numerical results

The composite used is a UD-CFRP with a "High Resistance" (HR) and an epoxy resin. The mechanical properties of the fibres and the matrix studied are given in Tab. 1.

Table 1: Material properties (fiber and matrix)

Property	Value
Carbon fiber HR [12]	
Fiber volume V_f [%]	60
Elasticity's modulus in the fibre direction $E_{f,l}$ [GPa]	230
Elasticity's modulus in the transverse direction $E_{f,t}$ [GPa]	15
Poisson's ratio υ_f [-]	0.3
Fibre shear modulus $G_{f,lt}$ [GPa]	50
Epoxy matrix [17]	
Elasticity's modulus E_m [GPa]	4.2
Poisson's ratio υ_m [-]	0.34
Matrix shear modulus G_m [GPa]	1.567

The standard thickness of a unidirectional ply of "High Resistance" (HR) carbon fibre is 0.13 mm [12]. The number of stacked plies varies from 20 to 40 plies in steps of 10 plies. The thickness of the plates studied therefore varies from 2.6 to 5.2 mm in steps of 1.3 mm. The dimensions of the plate are 100 x 31.4 mm (L x h). The plate has 50 elements horizontally and 20 elements vertically. The tool used is a 2-flute Tungsten Carbide end mill. The diameter of the mill D_c is 9.525 mm (3/8 inch). The properties of the plates and the tool studied, are listed in Tab.2.

Table 2: Plate and tool properties

Property	Value
Plate	
Thickness of a UD-CFRP ply e_p [mm]	0.13
Number of plies n_{plies}	20 – 30 – 40
Thickness of the plate e [mm]	2.6 – 3.9 – 5.2
Length of the plate L [mm]	100
Height of the plate h [mm]	31.4
Number of elements horizontally	50
Number of elements vertically	20
Tool	
Number of flutes	2
Cutting diameter of the tool D_c [mm]	9.525
Normal rake angle [°]	3

In terms of cutting conditions, the axial depth of cut ap was set at 10 mm. The radial depth of cut a_e is equal to half the plate thickness (variable between 1.3 and 2.6 mm). The cutting speed v_c is fixed at 5000 rpm. The feed per tooth f_z is variable between 0.02 and 0.1 mm/th in steps of 0.02 mm/th. These cutting parameters are listed in Tab.3.

Table 3: Cutting parameters

Property	Value
Axial depth of cut a_p [mm]	10
Radial depth of cut a_e [mm]	1.3 – 1.95 – 2.6
Cutting speed v_c [rpm]	5000
Feed per tooth f_z [mm/th]	0.02 – 0.04 – 0.06 – 0.08 – 0.1

The deformation is calculated for the various cases. Fig. 4 shows the deformation of the 2.6 mm thick plate when the tool enters the material at the top left corner. The shape of this deformation is similar for all the cases studied. Only the amplitude of the deformation varies and is explained below.

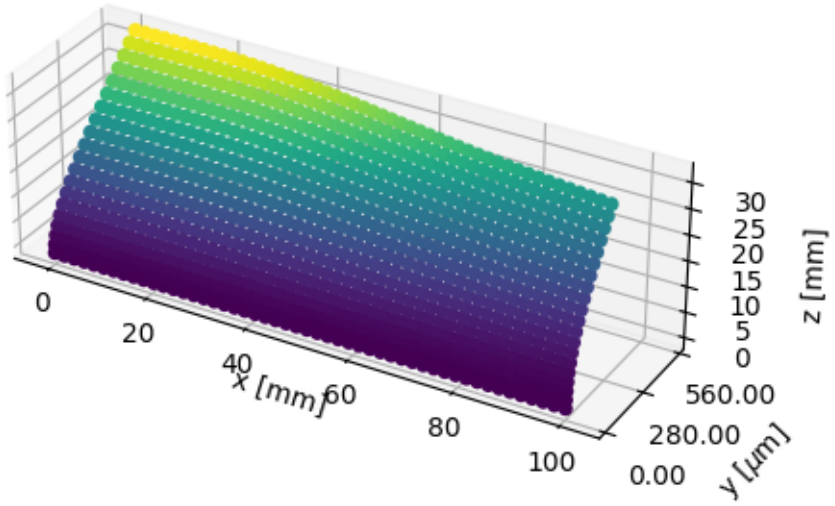

Figure 4: Deformation of the 2.6 mm plate with cutting tool at the upper left corner

Fig. 5 shows the average cutting force and the maximum deformation of a 2.6 mm plate as a function of the milling position. Fig. 5.a shows the maximum deformation for a 2.6 mm thick plate with a tooth feed variable between 0.02 mm/th and 0.1 mm/th in steps of 0.02 mm/th. The maximum deformation of the plate is reached at the ends of the plate (when x is equal to 0 or 100 mm). This deformation increases as the feed per tooth increases. It varies between 0.240 mm for a tooth feed of 0.02 mm/th and 0.494 mm for a tooth feed of 0.1 mm/th. This is because the average cutting force increases as the feed per tooth increases (Fig. 5.b). Between 0 and 50 mm, the cutting force increases. This is because the deformation decreases between 0 and 50 mm (Fig. 5.b), which increases the radial cutting depth ae and therefore the cutting force. Between 50 and 100 mm, the opposite effect occurs, as the deformation increases, resulting in a decrease in the radial cutting depth ae and therefore a reduction in the cutting force. The same trend can be observed for the other plate thicknesses.

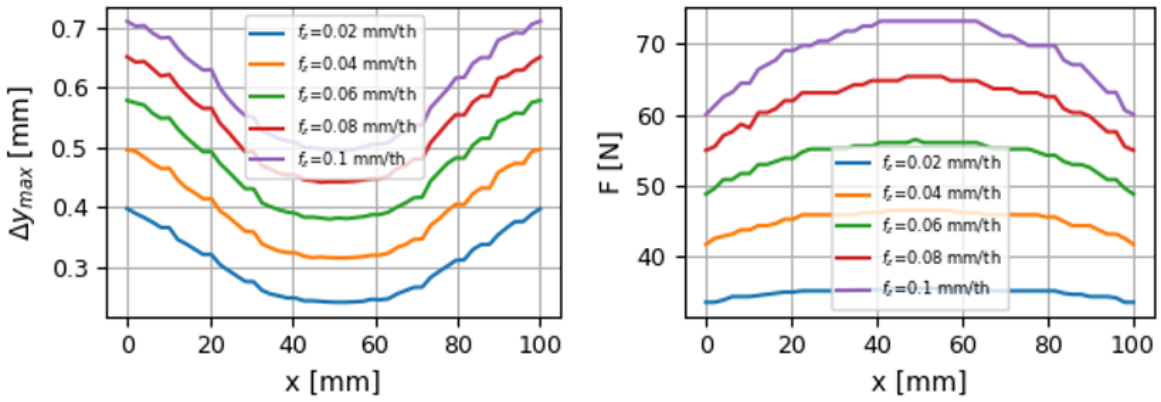

a) Maximum deformation b) Average cutting force

Figure 5: Spatial evolution for a 2.6 mm thick plate

Fig. 6 shows the spatial evolution of the average cutting force and maximum deformation for fixed cutting conditions (feed per tooth of 0.02 mm/th). The trends are similar to those shown in Fig. 5. Furthermore, the thicker the plate, the greater the cutting force, since the radial depth of cut is equal to half the plate thickness. Even if the cutting force increases, the maximum deformation decreases as the plate thickness increases. This is due to the increase in plate stiffness as plate thickness increases. The same trend can be observed for the other feed rate.

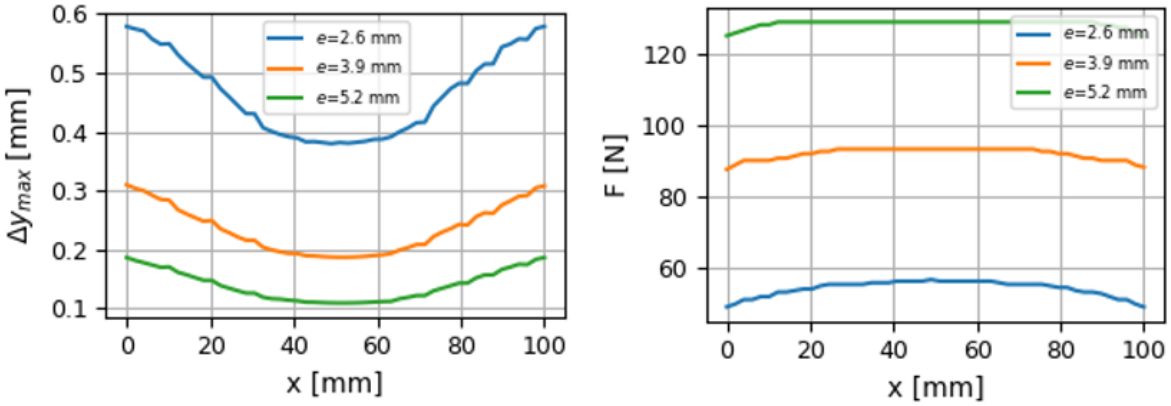

a) Maximum deformation b) Average cutting force

Figure 6: Spatial evolution for a feed rate of 0.6 mm/th

In conclusion, the behaviour of the plates for the different study cases is similar. The levels of cutting forces and deformation are different according to thickness and feed rate. However, they follow the same trends.

Conclusions

As FRPs are increasingly used materials, it is important to study their behavior during the thin plate milling operation. The main goal of this paper is to adapt models for calculating form error during thin metal plate milling to FRPs. The introduced modifications make it possible to calculate the form error for the case studied: a UD-CFRP laminate with all its plies oriented in the feed direction.

In addition to experimental validation, the outlook for this work is to improve the model to generalize the case studied. Indeed, the finite element model must be generalized for an anisotropic material (fiber orientation angle different from 0°) or for mirror laminate, an equivalent orthotropic material (as many plies in the ψ direction as -ψ). In addition, edge trimming operations, with the axis of the milling cutter perpendicular to the plate, need to be studied.

Acknowledgments

The authors would like to thank Région Wallonne for supporting this research as part of the MachFlexComp M-ERA.NET 2022 research project under grant 2210138.

References

[1] J. Du, M. Geng, W. Ming, W. He, and J. Ma, ‘Simulation machining of fiber-reinforced composites: A review’, *Int. J. Adv. Manuf. Technol.*, vol. 117, no. 1–2, pp. 1–15, Jul. 2021. https://doi.org/10.1007/s00170-021-07531-3

[2] I. Del Sol, A. Rivero, L. N. López de Lacalle, and A. J. Gamez, ‘Thin-Wall Machining of Light Alloys: A Review of Models and Industrial Approaches’, *Materials*, vol. 12, no. 12, Art. no. 12, Jan. 2019. https://doi.org/10.3390/ma12122012

[3] I. Llanos, A. Robles, J. Condón, M. Arizmendi, and A. Beristain, 'Deflection error modeling during thin-wall machining', *Procedia CIRP*, vol. 117, pp. 169–174, 2023. https://doi.org/10.1016/j.procir.2023.03.030

[4] E. Rivière-Lorphèvre, E. Filippi, and P. Dehombreux, 'Numerical Simulation of Machining Operations on Flexible Parts', *Key Eng. Mater.*, vol. 554–557, pp. 1984–1991, Jun. 2013. https://doi.org/10.4028/www.scientific.net/KEM.554-557.1984

[5] K. Kecik, R. Rusinek, J. Warminski, and A. Weremczuk, 'Chatter control in the milling process of composite materials', *J. Phys. Conf. Ser.*, vol. 382, no. 1, p. 012012, Aug. 2012. https://doi.org/10.1088/1742-6596/382/1/012012

[6] K. Ciecieląg and K. Zaleski, 'Milling of Three Types of Thin-Walled Elements Made of Polymer Composite and Titanium and Aluminum Alloys Used in the Aviation Industry', *Mater. 1996-1944*, vol. 15, no. 17, p. 5949, Sep. 2022. https://doi.org/10.3390/ma15175949

[7] Y. Song, H. Cao, W. Zheng, D. Qu, L. Liu, and C. Yan, 'Cutting force modeling of machining carbon fiber reinforced polymer (CFRP) composites: A review', *Compos. Struct.*, vol. 299, p. 116096, Nov. 2022. https://doi.org/10.1016/j.compstruct.2022.116096

[8] G. V. G. Rao, P. Mahajan, and N. Bhatnagar, 'Micro-mechanical modeling of machining of FRP composites – Cutting force analysis', *Compos. Sci. Technol.*, vol. 67, no. 3, pp. 579–593, Mar. 2007. https://doi.org/10.1016/j.compscitech.2006.08.010

[9] R. Rentsch, O. Pecat, and E. Brinksmeier, 'Macro and micro process modeling of the cutting of carbon fiber reinforced plastics using FEM', *Procedia Eng.*, vol. 10, pp. 1823–1828, Jan. 2011. https://doi.org/10.1016/j.proeng.2011.04.303

[10] D. Iliescu, D. Gehin, I. Iordanoff, F. Girot, and M. E. Gutiérrez, 'A discrete element method for the simulation of CFRP cutting', *Compos. Sci. Technol.*, vol. 70, no. 1, pp. 73–80, Jan. 2010. https://doi.org/10.1016/j.compscitech.2009.09.007

[11] H. N. Huynh, E. Rivière-Lorphèvre, F. Ducobu, A. Ozcan, and O. Verlinden, 'Dystamill: a framework dedicated to the dynamic simulation of milling operations for stability assessment', *Int. J. Adv. Manuf. Technol.*, vol. 98, no. 5–8, pp. 2109–2126, Sep. 2018. https://doi.org/10.1007/s00170-018-2357-3

[12] D. Gay, *Matériaux composites*, 6e éd. revue et augmentée. Paris: Lavoisier Hermès, 2015.

[13] O. C. Zienkiewicz, *The finite element method*, 3., Expanded and rev. Ed.. reprint. London Hamburg: McGraw-Hill, 1986.

[14] B. Castanié, C. Bouvet, and D. Guedra-Degeorges, 'Structures en matériaux composites stratifiés', *Concept. Prod.*, Oct. 2013. https://doi.org/10.51257/a-v2-bm5080

[15] R. Mullin, M. Farhadmanesh, A. Ahmadian, and K. Ahmadi, 'Modeling and identification of cutting forces in milling of Carbon Fibre Reinforced Polymers', *J. Mater. Process. Technol.*, vol. 280, p. 116595, Jun. 2020. https://doi.org/10.1016/j.jmatprotec.2020.116595

[16] Y. Altintaş and P. Lee, 'A General Mechanics and Dynamics Model for Helical End Mills', *CIRP Ann.*, vol. 45, no. 1, pp. 59–64, Jan. 1996. https://doi.org/10.1016/S0007-8506(07)63017-0

[17] P. D. Soden, M. J. Hinton, and A. S. Kaddour, 'Lamina properties, lay-up configurations and loading conditions for a range of fibre-reinforced composite laminates', *Compos. Sci. Technol.*, pp. 1011–1022, Mar. 1998. https://doi.org/10.1016/S0266-3538(98)00078-5